

Abstract

A new approach for development of seismic design parameters for newly developed seismic resistant systems is proposed by the Applied Technology Council (ATC) Project 63, in a program sponsored by the U.S. Federal Emergency Management Agency. The methodology is probability based, comprehensive and objective. Application of seismic parameters determined on this basis ensures acceptably low collapse probability of the designed structure. The basis of the approach is the collapse analysis of representative archetypical buildings, considering relatively large number of actual ground motion records. The method invokes a series of nonlinear static and dynamic analyses using numerical models that are calibrated to monotonic and cyclic experimental results. The seismic performance quantification is conducted by the statistical evaluation of the numerical results.

In this paper, the authors illustrate application of the ATC-63 method to a new light-framed steel building system, developed by Tipping Mar + Associates in California. The lateral resisting system consists of a steel corrugated sheet shear wall bracing system for use in mid-size residential and commercial structures.

Keywords: corrugated steel shear wall, seismic performance, statistical performance quantification, monotonic backbone curve estimation, pinching hysteretic behaviour, model calibration, pushover analysis, incremental dynamic analysis.

1 Introduction

When developing new seismic resistant structural system, its seismic performance shall be evaluated and quantified: most importantly, the seismic parameters – such as the behaviour factor, overstrength factor, etc. – that can be applied in practical design shall be reliably determined. The seismic performance is often studied on the element level by the help of cyclic tests. The quantification of seismic performance parameters such as the behaviour factor is then typically completed on an empirical

basis by analyzing the load capacity, local ductility, energy dissipation, and other factors, considering certain empirical limits for these parameters. Comparison to other well-studied structural systems may also guide us in the performance evaluation. However, the process of evaluating seismic performance factors for new structural systems requires significant judgment.

The Applied Technology Council (ATC) Project 63 proposes a new approach for to evaluate the adequacy of seismic performance factors and other code provisions for newly developed seismic-resisting systems [1]. The basis of the approach is the assessment of collapse performance of representative archetypical buildings, when subjected to a set of recorded ground motions. The method relies on a series of nonlinear static and dynamic analyses using numerical simulation models that are calibrated to monotonic and cyclic test results. The seismic performance quantification is conducted by the statistical evaluation of the numerical results. Application of seismic parameters determined on this basis ensures that the resulting structural system designed according to these provisions has an acceptably low collapse probability.

In this paper, the authors illustrate a practical application: light-framed steel buildings with a steel corrugated sheet shear-wall lateral-resisting system, shown in Figure 1, as developed by Tipping Mar + Associates, California [2]. The light-frame steel system is intended for use in mid-size residential and commercial structures. The proposed shear wall system utilizes low profile corrugated steel sheet as sheathing, which is fastened to cold-formed steel framing with screws. Vertical studs are located at every two feet (~ 61 cm); and horizontal end tracks are applied at the top and bottom of the wall. An experimental programme used to develop and validate the seismic performance of this system is described below. Based on the test results, nine assemblies are recommended for practical application, covering a wide range of load resistance demands. [2]

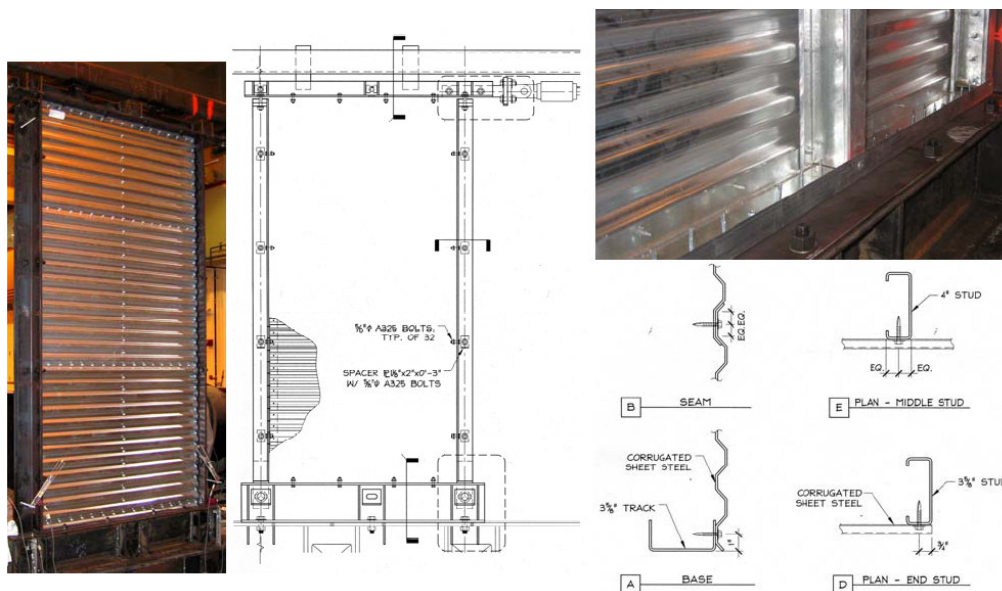


Figure 1: Shear wall configuration and test setup. [2]

Prior to the introduction of the performance estimation of the light frame steel wall system, the following American terms – that are not obvious or not used in Europe – have to be defined:

- *maximum considered earthquake, MCE*: the maximum earthquake effect considered in design; typically, the 2500-year return period ground motions. The *MCE* is structural period dependent and represented by the notation S_{MT} .
- *response modification factor, R*: analogous to the behaviour factor q , as defined in the Eurocode 8 Part 1 (EC8, [3]).
- *displacement modification factor, C_d* : analogous to the displacement factor q_d in EC8.
- *system overstrength factor, Ω_0* : analogous to the overstrength factor in EC8. Note that the Ω_0 factor reflects the summarized effect of material hardening, nominal vs. expected values of material properties, reserve capacity due to element overdesign and system overstrength, while EC8 distinguishes these sources of overstrength in separate factors.

These definitions are consistent and based on current U.S. seismic provision (e.g. ASCE 7-05 [4]). This terminology is used in this paper.

2 Seismic performance quantification by ATC-63

ATC-63 provides a comprehensive general framework for seismic performance evaluation of new systems. The methodology achieves the primary life safety performance objective by requiring an acceptably low probability of collapse of the seismic force resisting system for maximum considered earthquake (MCE) ground motions. It presumes that the structural system is clearly defined and so-called archetype buildings that well represent the application fields are determined. For the newly proposed steel wall building – on the basis of the archetype analysis –, the following common performance factors are estimated by the method:

- response modification factor, R , (EC8: behaviour factor, q),
- displacement modification factor, C_d , (EC8: q_d) and
- overstrength factor, Ω_0 , (EC8: overstrength factor).

The method consists of the following steps:

1. Multiple realizations of idealized archetypical lateral systems are designed, covering the expected range of building heights, bay widths, gravity load ratios, seismic design categories, etc. Typically 20-30 different building archetypes are de facto designed in accordance to design provisions and assuming certain performance parameters.
2. Experimental data, information on the actual monotonic and hysteretic behaviour of the dissipative elements are gathered and evaluated.
3. Analytical model of the building archetypes are developed and calibrated to experimental test data.
4. For each archetype building, non-linear static pushover analysis is used to determine the overstrength factor, and to characterize system global ductility.

5. Non-linear incremental dynamic analysis (IDA) is completed for each archetype, using 22 pairs of recorded ground motion defined by the ATC-63 document. The major outcomes of this analysis are the ground motion intensities that cause collapse of the archetype.
6. IDA results are used to generate a *fragility curve*, which describes the probability of building collapse as a function of ground motion intensity. The adjusted collapse margin ratio (ACMR) is calculated as the ratio of the median collapse intensity and MCE. If ACMR exceeds the minimum acceptable value given by ATC-63, the collapse probability is acceptably low¹ and the seismic performance factors assumed in the initial designs are deemed to be appropriate. The acceptable values of ACMR account for the uncertainties in the model, control of failure modes, quality of experimental data, etc. Systems with more underlying uncertainty are required to have larger ACMRs to meet requirements for probability of collapse. If the required ACMR is not met, the system must be redesigned, either by modifying the R-factor or refining design detailing requirements.

For further details on the ATC-63 methodology, please refer to [1], [5] and [6].

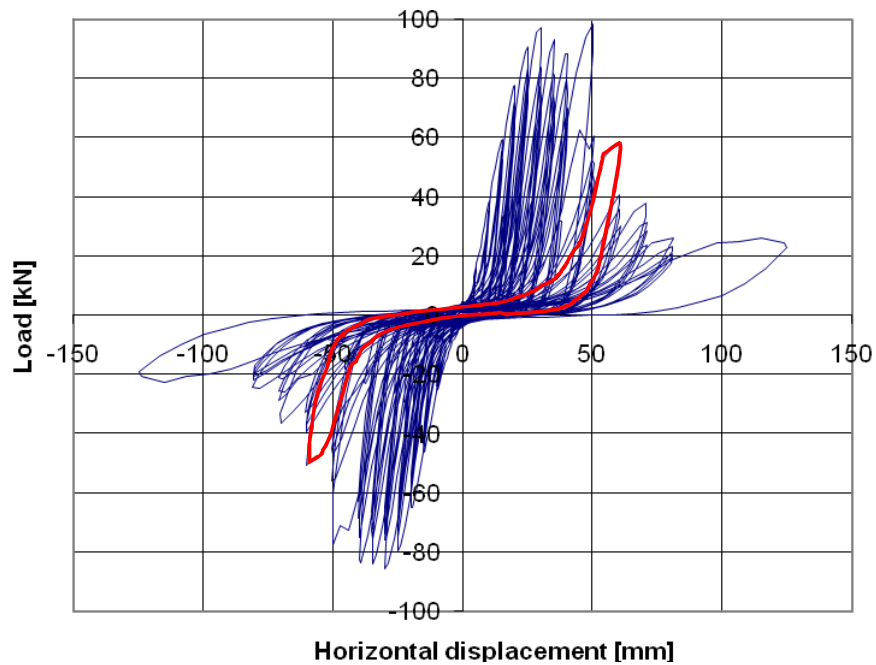


Figure 2: Typical hysteresis curve.
(one typical hysteresis loop is indicated by the red curve)

¹ In practice, an acceptably low probability of collapse is defined such that new structural systems have less than 10% probability of collapse under the *MCE* on average. No single archetype structure can have greater than 20% probability of collapse under the *MCE*.

3 Experimental results

Cyclic tests on 4-feet (~1.2 m) wide and 8-feet (~2.5 m) high corrugated panels (Figure 1) were completed by Stojadinovic et al. [2] at the University of California, Berkeley. Altogether, 44 specimens (24 groups) were tested to investigate six design parameters: 1) corrugated sheet thickness; 2) gauge of studs and tracks; 3) screw type/size; 4) fastener spacing; 5) inclusion of gypsum board; 6) one-sided or double-sided corrugated sheet application. No monotonic tests were completed and all tests used the AC154 loading protocol.

Figure 2 illustrates the typical hysteresis curve of the corrugated steel shear wall system. The pinching characteristics resulted from the failure mode of the screwed connection zone can be clearly observed in the hysteretic behaviour: bearing of the sheet, screw tilt and pull-out. Note that plate buckling and warping of the panel typically develops after the failure of the connection zones in the vicinity of the corners, and thus it hardly influences the load capacity.

The experimental research and its findings are detailed in [2].

4 Archetypical buildings

With certain aspects, the scope and application field of the steel shear wall system is similar to wooden shear walls (e.g. OSB panels). Based on this observation, in the archetypical building selection one may follow the OSB-panel example described in the ATC-63 document [1]. Accordingly, the following assumptions are made in the archetype definition:

- Two major building functions are distinguished: residential and commercial (Figure 3). The function also defines the plan and the size of the building. According to the function, two groups of archetypes, termed “performance groups”, are set up. Performance of the different groups can be evaluated independently.
- Number of storeys: 1 ~ 10. (Note that according to current U.S. codes [4], the system cannot be applied in buildings taller than 5 stories.)
- Seismicity: High. This corresponds to seismic design category (SDC) D in ASCE 7-05 and an MCE of 1.5g for short-period buildings. [4]
- Rectangular plan; the bracing wall system runs along the perimeter.
- With respect to the similarities to the wooden panel system [6], $R = 4\sim 5$ is expected. Initially, the archetypes are designed with $R = 4$, i.e. the purpose of this study is to confirm this value.

Although the archetypical buildings consist of shear walls and gravity system, the contribution of the columns to the lateral resistance is neglected and the total horizontal load is resisted by the wall. Therefore, only the shear wall is included in the analysis models. Based on the above design decisions, the required wall type and length is well defined for a given building size and mass.

The structural determinacy enables the simplified archetype definition. With the above aspects, altogether 13 archetypical buildings in two groups are defined and

designed (Table 1). For details on the design, refer to [6]. (The authors note that the final version of the ATC 63 guidelines requires a larger number of performance groups than those considered in this study. However, their inclusion is not expected to affect the conclusions.)

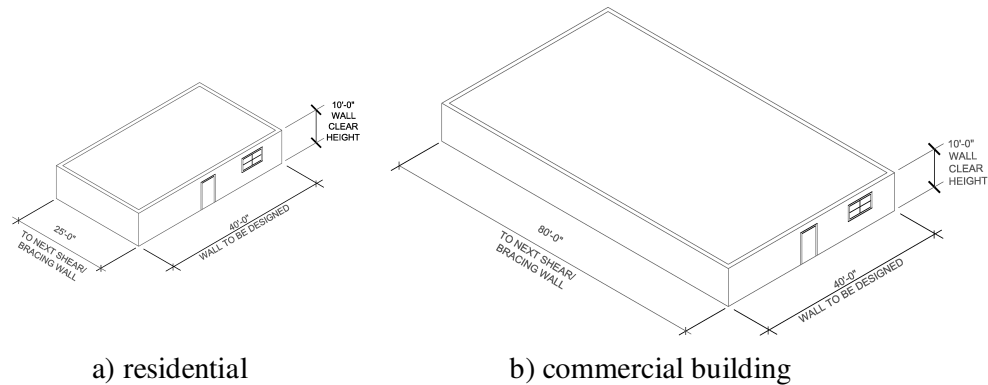


Figure 3: Archetypal buildings. [1]

R = 4 High seismic (SDC Dmax)

$$S_S = 1.5, S_1 = 0.9 (S_{DS} = 1.0, S_{D1} = 0.6)$$

Group	Archetype #	Storey #	Function	A_{floor} [m ²]	Weight [kN/m ²]	T_{design} [s]	S_{MT} [g]	C_s [-]	Design base shear force [kN]
I	1	1	commercial	149	1.45	0.16	1.50	0.25	53.4
	5	2	commercial	149	1.45	0.19	1.50	0.25	106.8
	9	3	commercial	149	1.45	0.26	1.50	0.25	160.1
II	2	1	1&2 family	46	0.5	0.112	1.50	0.25	5.6
	6	2	1&2 family	46	0.5	0.19	1.50	0.25	11.1
	10	3	multi-family	46	1.45	0.26	1.50	0.25	50.0
	13	4	multi-family	46	1.45	0.32	1.50	0.25	66.7
	15	5	multi-family	46	1.45	0.38	1.50	0.25	83.4
	17	6	multi-family	46	1.45	0.431	1.50	0.25	100.1
	18	7	multi-family	46	1.45	0.484	1.50	0.25	116.8
	19	8	multi-family	46	1.45	0.535	1.50	0.25	133.4
	20	9	multi-family	46	1.45	0.584	1.50	0.25	150.1
	21	10	multi-family	46	1.45	0.632	1.42	0.237	158.3

S_S : MCE spectrum ordinate (spectral acceleration) in the short-period region; S_1 : MCE spectral acceleration at $T = 1$ sec; S_{DS} : design spectral acceleration in the short-period region; S_{D1} : design spectral acceleration at $T = 1$ sec; A_{floor} : floor area tributary to the wall; $Weight$: seismic weight; T_{design} : fundamental period of the building, based on ASCE7-05; S_{MT} : MCE spectral acceleration at T_{design} ; C_s : base shear force coefficient (ratio of base shear force to seismic weight)

Table 1: Defined archetypes.

5 Numerical modelling and calibration

5.1 Global numerical model of archetypes

The software selected for the structural analysis is the *Open Systems for Earthquake Engineering Simulation* (OpenSees, [7]), an open-source software platform developed by the Pacific Earthquake Engineering Research Center.

A single frame of the building is represented by 2D truss structure shown in Figure 4. The shear walls are modelled by single diagonal uniaxial truss element at each storey, as shown in the figure. A non-linear material model is applied for this element, which has been calibrated to the experimental data provided by [2]; other elements (including beams, columns and leaning column) are associated with elastic materials. Connections between every element are pinned. Consequently, possible contributions from the columns and beams are conservatively ignored. Leaning column (pinned, rigid elements) is used to account for the masses that – in a vertical sense – are not directly transferred to the columns of braced bay, but are tributary to the bracing wall system with respect to lateral load bearing.

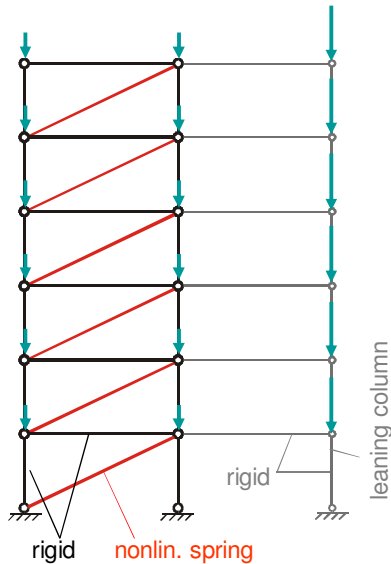


Figure 4: Global archetype model.

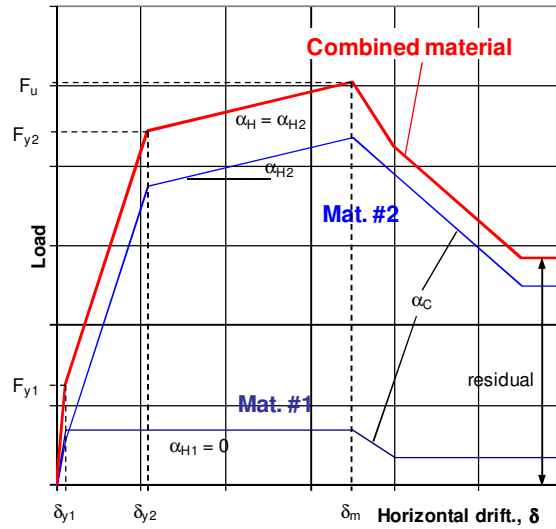


Figure 5: Combined material.
(monotonic backbone curve)

The monotonic as well as the cyclic behaviour (Figure 6; blue and red curves, respectively) of the wall shall be reflected by the substitutive link element. Monotonic behaviour is represented by the so-called backbone curve. Hysteretic response is derived from the monotonic curve by mean of cyclic degradation parameters. The test results (referring back to Figure 2) show that the behaviour is non-linear from the very beginning, which results in an unloading stiffness steeper than the effective (secant) initial stiffness. In order to capture this behaviour, two materials are combined in parallel, resulting in a short, steep initial part, as shown in

Figure 5. To simulate pinching behaviour and cyclic degradation, the Ibarra-Medina-Krawinkler [8] model is applied (Figure 6). The resulting material model can be described by 15 independent parameters (Figure 5-6):

- a) parameters for the backbone curve (yield and ultimate loads F_{y1} , F_{y2} , F_u and corresponding displacements δ_{y1} , δ_{y2} , δ_m , capping slope α_c and residual r);
- b) pinching parameters (α_p and β_p);
- c) cyclic degradation parameters (c , γ_A , γ_S , γ_D , γ_K).

The estimation of these parameters is described next.

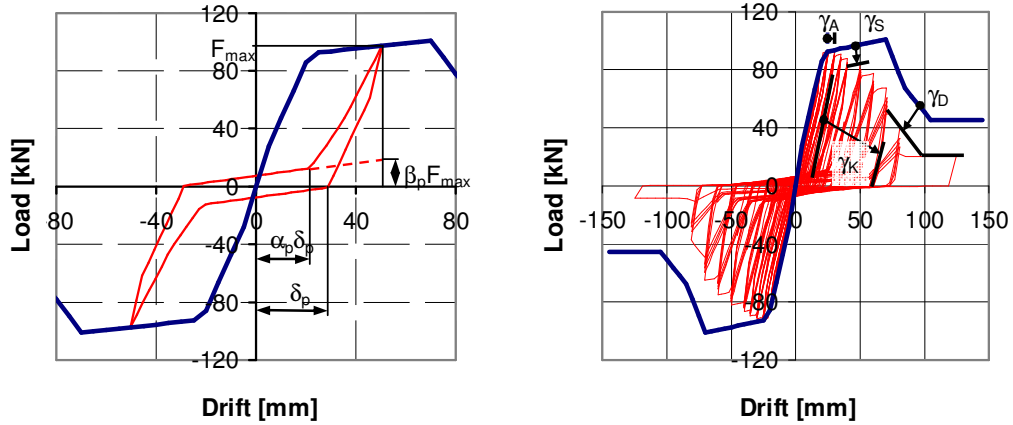


Figure 6: Ibarra-Medina-Krawinkler [8] material model.

5.2 Estimation of monotonic backbone curve

In order to achieve an analytical model that reliably and accurately captures the actual behaviour, accurate estimation of the monotonic backbone curve is necessary. The model calibration cannot be completed only on the basis of cyclic test results, as those are dependent on the load protocol. Calibration of the analysis model is complicated by the fact that the same cyclic results can be obtained with different sets of capping point locations and degradation properties (i.e. a large number of possible solutions may exist). The challenge is to back-calculate a set of parameters that are generally applicable for any loading history.

Typically, the backbone curve parameters are outcomes of monotonic test results. Since monotonic tests were not conducted on the steel panel walls, in this case the backbone curve is evaluated by separate non-linear static analysis. The shear walls are modelled in ANSYS [9], using shell elements and non-linear springs to represent the sheathing and the screw connections, respectively (Figure 7). The ultimate load of one screw is derived from preliminary analyses and test results available in literature and the characteristic behaviour is adjusted on the basis of comparison of the tested and simulated overall behaviour (Figure 8). In the adjustment, it is assumed that up to a certain level of deformation (e.g. 35 mm in case of Figure 8) the cyclic envelope curve approaches the monotonic backbone curve, i.e. the cyclic degradation is negligible in the early plastic stage. With this circumstances, the non-

linear static analysis provides an upper bound for the capping point (in terms of both displacements and resistance), but does not give information on the post-capping behaviour; i.e. in this way, the parameters F_{y1} , F_{y2} , F_u , δ_{y1} , δ_{y2} and δ_m can only be estimated. Testing the actual screw connections would enable more accurate analysis capturing a wider range of the backbone curve.

The ANSYS model also helped the authors to better understand the overall wall behaviour. The results indicate that the corrugated sheet remains elastic even at large deformations and that the connection zone controls the failure initiation with the modes of bearing, tilting and finally pull-out. The screw pull-out is accompanied by the increased shear buckling and warping deformations of the panel.

The analysis also confirmed that connection failure is the governing failure mode of the longer wall, too, as observed in the short test panel. Although one may expect an increasing role of overall shear buckling in the long wall, the change in buckling capacity is negligible beyond an aspect ratio of 1. The numerical study helps to justify the assumption that the shear panel strength is linearly related to its length. [6]

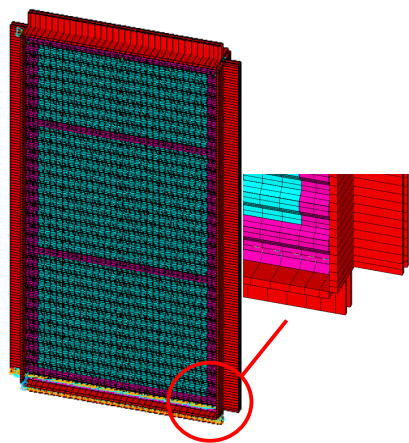


Figure 7: Detailed FE model.

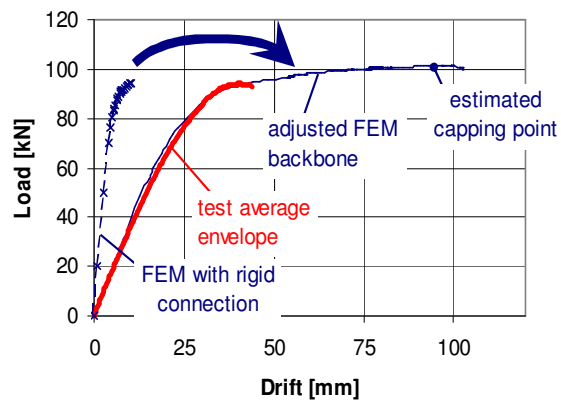


Figure 8: Model adjustment.

5.3 Genetic algorithm for determination of model parameters

Given that the backbone curve is known up to the capping point and some of the parameters can be excluded, the unknown parameters to calibrate are the capping slope α_c , the residual r , the pinching (α_p , β_p) and three of the cyclic degradation parameters (γ_A , γ_B , γ_D). Calibration is completed on the tested configurations, using single shear wall element.

To overcome the indeterminacy of the parameter calibration process, a genetic algorithm (GA) is applied for determining the post-capping and cyclic response parameters. The objective function is the weighted sum of square errors of the tested and calibrated load values for given displacement. The error function is weighted with the displacements in order to increase the importance of the final – degraded – parts of the hysteresis curve.

Using the GA structure and parameters given in Figure 9, a population size of 20 is found eligible. As Figure 10 proves, after approximately 100 generations an optimal solution can be found with this parameter set. The authors emphasize that a single optimal solution (referred to as uniform model) that can be reliably applied for most of the wall configurations is found (Figure 11); the only changing parameters (F_{y1} , F_{y2} , F_u) are related to the load ordinates of the backbone curve.

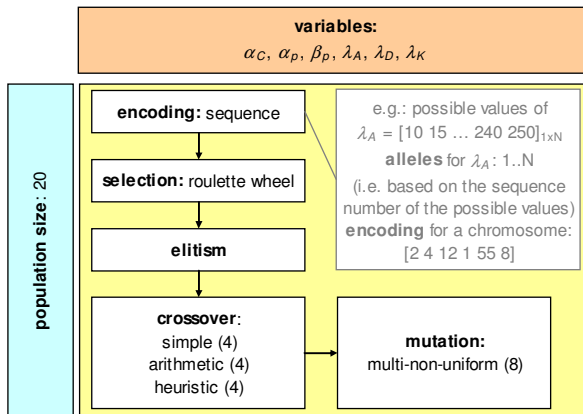


Figure 9: Structure of genetic algorithm.

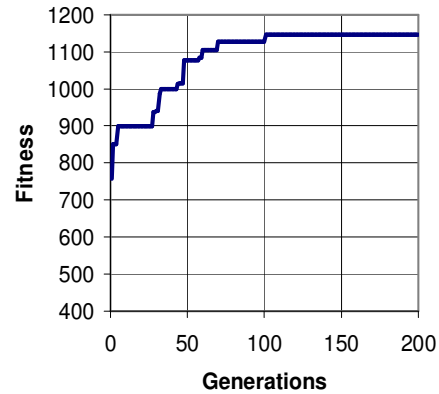
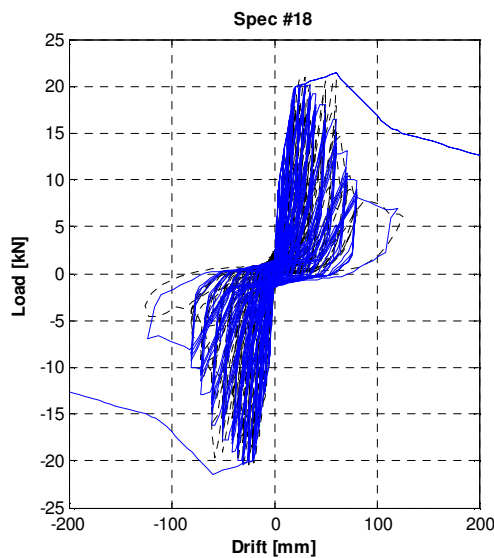


Figure 10: Convergence of optimization.



	Uniform
F_{y1}	$= \alpha_{F,i} F_{ASD}^{(8)}{}_{y1} = \alpha_{F,i} 25.0$
e_{y1}	3.99
F_{y2}	$= \alpha_{F,i} F_{ASD}^{(8)}{}_{y2} = \alpha_{F,i} 56.0$
e_{y2}	20.00
F_{y3}	$= \alpha_{F,i} F_{ASD}^{(8)}{}_{y3} = \alpha_{F,i} 60.0$
$e_{y3} (\delta_{cap})$	60.00
α_{t2}	0.00
α_C	-0.05
$\alpha_{C,ratio}$	1.00
α_{pinch}	0.60
β_{cap}	0.21
c	1.00
λ_S	∞
λ_K	20.0
λ_A	20.0
λ_D	20.0
r	0.65

$$\alpha_{F,i} = \frac{F_{ASD}^{(i)}}{F_{ASD}^{(8)}}$$

$F_{ASD}^{(i)}$: ASD strength of the i^{th} group

Figure 11: Calibrated uniform model.

For the actual archetypes, the calibrated model has to be extrapolated with proper transformation to the actual wall length (walls used in archetypes are longer than 4 ft). As mentioned in the previous section, the numerical analysis confirmed that the shear panel strength is linearly related to its length. Based on this observation, the

calibrated model can be easily extrapolated to the actual dimensions in the archetypes.

Also note that numerical modelling and calibration possibly includes some uncertainties; the ATC method enables the consideration of such variability when selecting the allowable ACMR values.

6 Analysis and evaluation of archetypical buildings

6.1 Pushover analysis

The purpose of the pushover analysis is two-fold: a) firstly, the global ductility and the system overstrength can be calculated for the archetype system; b) secondly, the global failure mechanism can be studied.

Conventional pushover analysis is done for each archetype, using the code load distribution. Buildings are modelled using material and geometric non-linearities as described above. The analysis is displacement-controlled.

R = 4 High seismic (SDC Dmax)

$$S_3 = 1.5, S_1 = 0.9 (S_{DS} = 1.0, S_{D1} = 0.6)$$

Archetype	Storey #	Function	Ω_0 [-]	μ_c [-]	SSF [-]	S_{MT} (T_{design}) [g]	SF_{anchor} [-]	β_{tot} [-]	\hat{S}_{CT} [g]	CMR [-]	ACMR [-]		ACMR limit [-]	check (pass/fail)
1	1	commercial	2.38	6.25	1.31	1.50	2.10	0.70	2.79	1.86	2.44	>	1.80	Pass
5	2	commercial	2.40	4.37	1.26	1.50	1.97	0.70	2.93	1.95	2.46	>	1.80	Pass
9	3	commercial	2.39	3.36	1.22	1.50	1.88	0.70	3.04	2.03	2.47	>	1.80	Pass
Mean											2.46	>	1.80	Pass
2	1	1&2 family	9.91	6.31	1.31	1.50	2.60	0.70	4.85	3.24	4.24	>	1.80	Pass
6	2	1&2 family	4.91	4.95	1.27	1.50	1.97	0.70	4.44	2.96	3.76	>	1.80	Pass
10	3	multi-family	2.52	4.06	1.25	1.50	1.88	0.70	3.34	2.23	2.78	>	1.80	Pass
13	4	multi-family	2.56	3.00	1.20	1.50	1.95	0.70	3.01	2.01	2.41	>	1.80	Pass
15	5	multi-family	2.57	2.72	1.19	1.50	2.00	0.70	3.08	2.05	2.44	>	1.80	Pass
Mean											3.13	>	1.80	Pass
17	6	multi-family	2.57	2.48	1.17	1.50	2.05	0.70	2.98	1.98	2.32	>	1.80	Pass
18	7	multi-family	2.08	2.40	1.17	1.50	2.02	0.70	2.97	1.98	2.32	>	1.80	Pass
19	8	multi-family	2.34	2.34	1.18	1.50	2.14	0.70	2.79	1.86	2.19	>	1.80	Pass
20	9	multi-family	2.56	2.35	1.21	1.50	2.40	0.70	2.61	1.74	2.11	>	1.80	Pass
21	10	multi-family	2.42	2.31	1.22	1.42	2.44	0.70	2.30	1.62	1.97	>	1.80	Pass
Mean											2.65	>	1.80	Pass

S_3 : MCE spectrum ordinate (spectral acceleration) in the short-period region; S_1 : MCE spectral acceleration at $T = 1$ sec; S_{DS} : design spectral acceleration in the short-period region; S_{D1} : design spectral acceleration at $T = 1$ sec; Ω_0 : overstrength factor; μ_c : ductility ratio; SSF: spectral shape factor; S_{MT} : MCE spectral acceleration at T_{design} ; SF_{anchor} : scaling factor to anchor the time-history data at T_{design} ; β_{tot} : total uncertainty; \hat{S}_{CT} : median collapse intensity; CMR: collapse margin ratio; ACMR: adjusted collapse margin ratio

Table 2: Results of archetype analysis.

The major results are summarized in Table 2. Figure 12 illustrates the resulting typical capacity curve (base shear vs. roof displacement). The figure also demonstrates the definition and calculation of Ω_0 and the representative displacement values (δ_y , δ_u), as well as the ductility ratio μ_c . As for the steel shear wall, the calculated overstrength factor falls into the range of 2.4 ~ 2.6; i.e. applying such overdesign for the non-dissipative elements will assure the proper failure mechanism. (Note that the overstrength derived from pushover analysis is – although obviously related – not necessarily equal to the overstrength factor used in design. For this reason, different notations are typically applied.) Large variation can be observed in the ductility ratio with values 2.7 ~ 6.3. The tendency suits to the experienced differences in the local ductility of the different wall configurations. Note that the final version of ATC-63 uses a different definition for the ductility ratio, by which the presented results would be slightly different.

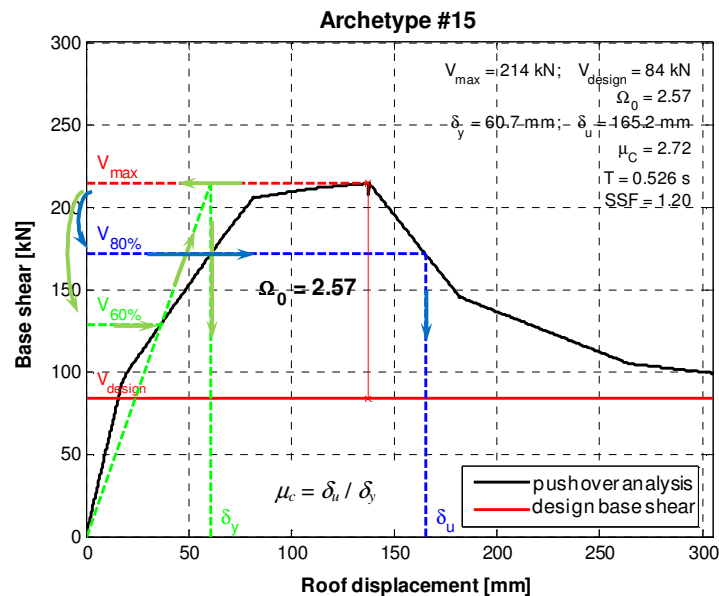


Figure 12: Capacity curve.

Based on the ductility ratio and the fundamental period of the structure, the so-called *spectral shape factor*, SSF can be determined. This factor reflects that the spectral shape may highly differ from the design spectrum in case of rare ground motions. The ATC 63 method for determination of the SSF accounts for the ductility of the archetype system and representative spectral shape of rare ground motions in the seismic design category of interest. [1]

6.2 Incremental dynamic analysis

The goal of the incremental dynamic analysis (IDA) is to predict the ground motion intensity corresponding to the collapse of the structure (e.g. global instability). Normalized ground motion records are gradually scaled up to the collapse level. (According to the ATC-63, ground motion intensity is defined as the spectral

acceleration S_{CT} at the fundamental period of the building – the spectrum is calculated for the seismic record set under consideration. For the scaling method, see [1] or [6].) As typical outcome of IDA, a series of interstorey drift vs. intensity curves shown in Figure 13 is found (one curve indicates IDA with one ground motion record). Global instability is numerically indicated as the nearly horizontal branch of the curve.

ATC-63 prescribes 22 pairs of ground motion records [1]. Each archetype has to be analyzed with the whole record set. For each seismic record the collapse intensity is determined; the median collapse intensity of the 44 records is then calculated for every archetype.

The so-called *fragility curve* (showing the probability of collapse – intensity relation) can be derived as the cumulative distribution of the collapse intensities associated with each record (Figure 14). Log-normal curve can be fit to the discrete values. The median value of this curve defines \hat{S}_{CT} , which can be normalized by S_{MT} to determine the collapse margin ratio *CMR*.

The results naturally include the record-to-record variability. The further uncertainties (e.g. in modelling, quality of test results, etc.) as well as the mentioned deviation in the spectral shapes can be taken into account by a simplified procedure. To account for spectral shape, the fragility curve is directly modified by the *SSF*. The *adjusted collapse margin ratio*, *ACMR* is the product of the *CMR* and the *SSF*. The other uncertainties are covered by the proper selection of allowable *ACMR* values. This limit depends on the total uncertainty β_{tot} that integrates the different sources of variability. Judgement is guided by quality categories in ATC-63: regarding to experimental data, modelling, etc., information and results of the shear wall study is rated as ‘*B (good)*’.

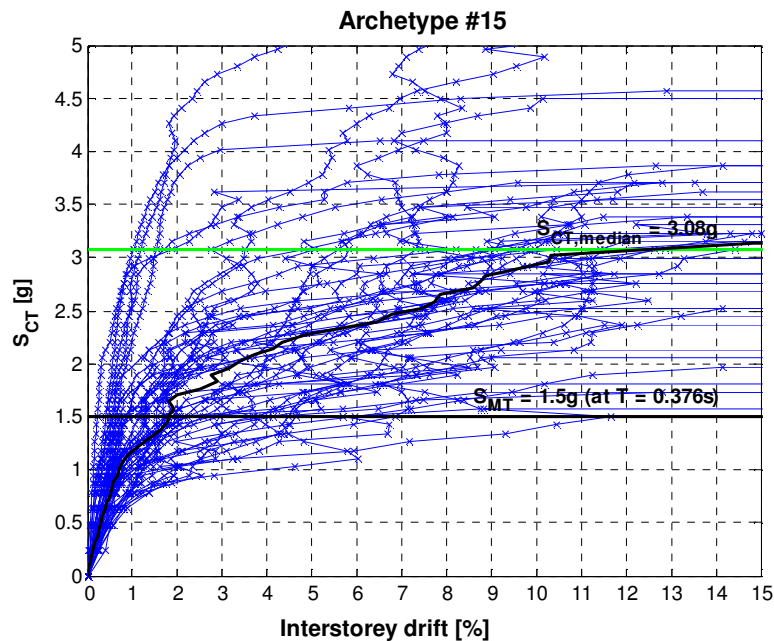


Figure 13: IDA curves for 44 records.

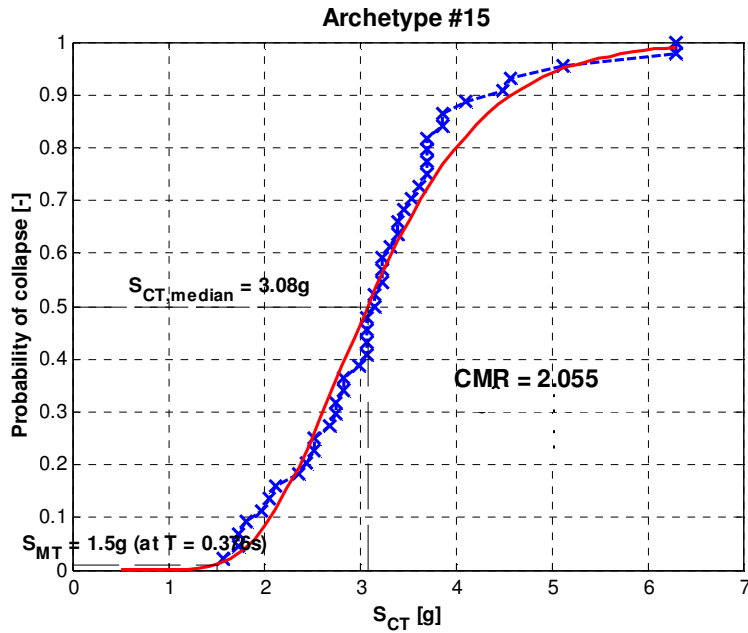


Figure 14: Typical fragility curve.

6.3 Seismic performance

The acceptability of the new structural system is judged by comparison of the computed *ACMRs* to the acceptable *ACMR* specified in the ATC-63 document. These acceptable *ACMR* are defined such that each archetype must have less than 20% probability of collapse under the MCE. In addition, the average for each performance group must meet the 10% probability of collapse criteria. As Table 2 shows, the required *ACMR* values are met at both the individual and group level; consequently, the initially assumed response modification factor ($R = 4$) is deemed to be appropriate. Note that if these criteria are not met, one has to restart the archetype design with decreased R value.

Per definition of ATC-63, the displacement modification factor, C_d equals to R . (Note that this assumption is typically incorrect in the short period range.)

The studied steel shear wall system shows similarities to the wooden light-frame system of [1] on the component as well as global level. On the component level, both systems are characterized by the pinching hysteresis behaviour. The capacity (needless to say, with different dimensions) and the ductility are also comparable. The similarities in the global behaviour are confirmed by the IDA results. [6]

7 Concluding remarks

The ATC-63 seismic performance evaluation method was presented through a practical example of steel shear wall system. The methodology is comprehensive and relatively objective; nevertheless, it is obvious from this example that

completion of such calculation can be extremely time-consuming (model calibration, large number of non-linear dynamic analysis). Note that seismic parameters determined by the methodology can be applied in practical design (and included in relevant building code documents) after peer review and authorization only.

It has to be emphasized that the discussed example is not complete, and thus, general conclusions cannot be drawn for the seismic parameters of the shear wall. Low seismicity case and influence of further – non-engineered – elements (e.g. finishing, compartment walls, etc.) are not investigated. Furthermore, contribution of the non-dissipative components is neglected, though they may directly or indirectly (via the internal force redistribution) improve the cyclic behaviour.

Acknowledgement

The authors express their thanks to The Thomas Cholnoky Foundation for sponsoring Laszlo Vigh's study sojourn at Stanford University, in the framework of the Dr. Imre Koranyi Scholarship.

References

- [1] "ATC-63: Recommended Methodology for Quantification of Building System Performance and Response Parameters", 90% Draft, Applied Technology Council, Redwood City, CA, 2008.
- [2] Stojadinovic, B., Tipping, S., "Structural testing of corrugated sheet steel shear walls", Research report, University of California, Berkeley, 2007.
- [3] "MSZ EN1998:2005 Eurocode 8: Design of structures for earthquake resistance – Part 1: General rules, seismic actions and rules for buildings", 2005.
- [4] "ASCE 7-05: Minimum Design Loads for Buildings and Other Structures", American Society of Civil Engineers, Reston, VA, 2005.
- [5] Deierlein, G.G., Liel, A.B., Haselton, C.B., Kircher, Ch.A., "Assessing Building System Collapse Performance and Associated Requirements for Seismic Design", Proc. SEAOC 2007 Convention, 2007.
- [6] Vigh, L.G., Deierlein, G.G., Miranda, E., Liel, A., Tipping, S., "Seismic performance of steel corrugated shear wall", Research report, Stanford University, 2008 (in preparation).
- [7] "OpenSees: Open Systems for Earthquake Engineering Simulation", <http://opensees.berkeley.edu>.
- [8] Ibarra, L., Medina, R., Krawinkler, H., "Hysteretic models that incorporate strength and stiffness deterioration", Eq. Eng. and Struct. Dynamics, Vol 34, No.12, pp.1489-1511, 2005.
- [9] "ANSYS Structural analysis guide", online documentation. ANSYS Inc.